Published in final edited form as:
J Phys Chem B. 2010 September 30; 114(38): 12416–12426. doi:10.1021/jp106113h.

The Intramolecular Charge Transfer State in Carbonyl-Containing Polyenes and Carotenoids

Miriam M. Enriquez, **Marcel Fuciman**, **Amy M. LaFountain**, **Nicole L. Wagner**, **Robert R. Birge***, and **Harry A. Frank***
Department of Chemistry, University of Connecticut, U-3060, 55 North Eagleville Road, Storrs, CT 06269-3060, USA

Abstract

Numerous femtosecond time-resolved optical spectroscopic experiments have reported that the lifetime of the low-lying S_1 state of carbonyl-containing polyenes and carotenoids decreases with increasing solvent polarity. The effect becomes even more pronounced as the number of double bonds in the conjugated π-electron system decreases. The effect has been attributed to an intramolecular charge transfer (ICT) state coupled to S_1, but it is still not clear what the precise molecular nature of this state is, and how it is able to modulate the spectral and dynamic properties of polyenes and carotenoids. In this work we examine the nature of the ICT state in three substituted polyenes: crocetindial, which contains two terminal, symmetrically-substituted carbonyl groups in conjugation with the π-electron system, 8,8'-diapocarotene-8'-ol-8-al, which has one terminal conjugated carbonyl group and one hydroxyl group, and 8,8'-diapocarotene-8,8'-diol, which has two terminal, symmetrically-positioned, hydroxyl groups but no carbonyls. Femtosecond time-resolved optical spectroscopic experiments on these molecules reveal that only the asymmetrically substituted 8,8'-diapocarotene-8'-ol-8-al exhibits any substantial effect of solvent on the excited state spectra and dynamics. The data are interpreted using molecular orbital theory which shows that the ICT state develops via mixing of the low-lying S_1 (2^1A_g-like) and S_2 (1^1B_u-like) excited singlet states to form a resultant state that preferentially evolves in polar solvent and exhibits a very large (~25D) dipole moment. Molecular dynamics calculations demonstrate that the features of the ICT state are present in ~20 fs.

Keywords

carotenoid; ICT state; excited state kinetics; molecular orbital theory; polyene spectroscopy

Introduction

One-photon electronic transitions to and from the ground state, S_0, to the lowest-lying excited state, S_1, of polyenes and carotenoids are forbidden due to the fact that both states are characterized by the same A_g^- symmetry representation.[1–5] The forbiddenness of this transition manifests itself in a very low quantum yield of emission from S_1, and an insensitivity to solvent environment of the S_1 energy and lifetime.[6–8] However, for polyenes and carotenoids possessing a carbonyl group in conjugation with the π-electron

*Authors to whom correspondence should be addressed: Robert R. Birge and Harry A. Frank, Department of Chemistry, 55 North Eagleville Road, University of Connecticut, U-3060, Storrs, CT 06269-3060. rbirge@uconn.edu and harry.frank@uconn.edu.

Supporting Information Available
Figures S1, S2 and S3 are available as supporting information. This information is available free of charge via the Internet at http://pubs.acs.org.

system, a large effect of solvent on the lifetime and $S_1 \rightarrow S_n$ excited state absorption (ESA) spectra has been reported.[9–15] Femtosecond time-resolved optical spectroscopic experiments on carbonyl-containing molecules having different π-electron conjugation lengths have demonstrated an increasing effect of solvent as the number of conjugated double bonds, N, in the π-electron system decreases.[12,13,15] The effect has been attributed to an intramolecular charge transfer (ICT) state that is coupled to S_1 and whose energy can be modulated by the polarity of the solvent.[8–10] Yet, apart from the obligatory presence of a carbonyl, it is still not clear what the molecular nature of the ICT state is, and how it controls the spectral and dynamic properties of polyenes and carotenoids. Various suggestions regarding the molecular basis of the ICT state include it being a separate electronic state from S_1,[9,16–19] quantum mechanically mixed with S_1,[20,21] or S_1 with a large intrinsic dipole moment.[22]

In this paper we examine of the nature of the ICT state in three substituted polyenes having seven conjugated carbon-carbon double bonds (Fig. 1). The molecules are crocetindial, which contains two terminal, symmetrically-substituted carbonyl groups in conjugation with the π-electron system, 8,8'-diapocarotene-8'-ol-8-al, which has one terminal conjugated carbonyl group and, on the other end of the molecule, one hydroxyl group, and 8,8'-diapocarotene-8,8'-diol, which has two terminal, symmetrically-positioned, hydroxyl groups and no carbonyls. Femtosecond time-resolved optical spectroscopic experiments on these molecules show that only the asymmetrically substituted 8,8'-diapocarotene-8'-ol-8-al exhibits any substantial effect of solvent on its ESA spectra and dynamics. The data are interpreted using molecular orbital theory which has revealed that the ICT state evolves via mixing of the low-lying 2^1A_g-like and 1^1B_u-like ππ* excited singlet states as a result of excited state bond order reversal. The resultant state preferentially evolves in polar solvent and exhibits a very large dipole moment (~25D). Molecular dynamics calculations indicate that the key properties of the ICT state are present after approximately 20 fs.

Experimental Methods

Crocetindial was obtained as a dry solid from Dr. Razi Naqvi. A solution of crocetindial in 2 mL of methanol (Fisher Scientific) having an optical density of ~2 in a 1 cm cuvette measured at its longest wavelength vibronic band was reacted with sodium borohydride (Acros Organics) by adding a few small crystals of the reducing agent to the solution. Within a few seconds the sample was transferred into a vial containing 4 mL of methyl-*tert*-butyl ether (MTBE, Fisher Scientific) and water (Sigma-Aldrich) (1:1, v/v). The polyenes moved readily into the ether layer, while the sodium borohydride remained dissolved in the aqueous phase, thus stopping the reaction. The ether layer was evaporated to dryness, and the remaining residue was redissolved in acetonitrile (Fisher Scientific) and injected into a Millipore Waters 600E high-performance liquid chromatograph (HPLC) employing either a Phenomenex Luna 5μ silica (250 × 4.6 mm) analytical column or a Waters Sunfire silica OBD (5μm, 19 × 100 mm) preparative column and a Waters 2996 single diode-array detector. The mobile phase consisted of a linear gradient from 90% hexanes (Fisher Scientific) and 10% acetone (Fisher Scientific) to 80% hexanes and 20% acetone over 20 minutes at a flow rate of either 1mL/ min (analytical column) or 7 mL/min (preparative column). HPLC peaks corresponding to unreacted crocetindial, 8,8'-diapocarotene-8'-ol-8-al, and 8,8'-diapocarotene-8,8'-diol (Fig. 1) were collected, dried under a gentle stream of gaseous nitrogen, and stored at −80°C. For the spectroscopic experiments, the molecules were dissolved in solvents having similar polarizabilities, R(n), but different polarities, P(ε): hexane (P(ε)=0.229, R(n)=0.228, Fisher Scientific), acetonitrile (P(ε)=0.921, R(n)=0.210, Fisher Scientific), and methanol (P(ε)=0.913, R(n)=0.203, Aldrich Chemicals).

Steady-state absorption spectra were recorded using a Varian Cary 50 UV-visible spectrophotometer and fluorescence measurements were carried out using a Jobin-Yvon Horiba Fluorolog-3 equipped with a Hamamatsu R928P detector and a 450 W ozone-free Osram XBO xenon arc lamp. Excitation and emission monochromator slits were set to a bandpass of 10 nm and 2.5 nm for fluorescence measurements and 2.5 nm and 10 nm for excitation measurements. The fluorescence spectra were corrected for the instrument response function using a correction factor file generated from a standard lamp.

Femtosecond time-resolved transient absorption measurements were made using a spectrometer system based on an amplified, 1 kHz Ti:Sapphire tunable laser (Spectra-Physics) as previously described.23 Pump pulses having a duration of ~60 fs were obtained by second harmonic generation using 0.7 mm Type I BBO crystal with resulting wavelength of 406 nm. Probe laser pulses used white light continuum between 450 – 800 nm generated by crystal from Ultrafast Systems LLC. A charge-coupled detector S2000 with a 2048 pixel array from Ocean Optics was used for detection. The planes of polarization of the pump and probe beams were set at the magic-angle (54.7°) relative to each other and the recorded signals were averaged over 5 second time intervals. All three samples were pumped at 406 nm. The energy of the pump beam was 1 μJ/pulse in a spot size of 1 mm diameter corresponding to an intensity of ~2.0×10^{14} photons/cm^2 per pulse. The full width at half maximum of the cross correlation in methanol for excitation pulses at 485 nm and probe pulses at 565 nm was determined to be ~170 fs according to the procedure of Ziolek *et al*.24 and was assumed to be same for other solvents due to the similarity of polarizability factors. The samples were adjusted to an optical density between 0.4 and 0.6 at the excitation wavelength in a 2 mm path length cuvette. Steady-state absorption spectra of the samples were taken before and after every transient experiment to ensure no sample degradation had occurred. Chirp correction of the transient absorption spectra was accomplished using Surface Explorer Pro (v.1.1.0.17) software (Ultrafast Systems LCC). Global fitting analysis was carried out using ASUfit version 3.0 software. The quality of the fit was evaluated based on the residual matrix and χ^2 probability distribution function.

Theoretical Methods

Molecular orbital theory

Vacuum calculations were carried out using MNDO-PSDCI,25 SAC-CI26–31 and EOM-CCSD32–35 methods. Solvent effect calculations were executed using the SCRF keyword as implemented in Gaussian 09.36 Each calculation was run using the integral equation formalism variant polarizable continuum model (IEFPCM) method with configuration interaction singles (CIS).37–42 Equilibrium state-specific solvation was accomplished using an external iteration approach with a Dunning/Huzinaga43 full double zeta basis set (D95). Semiempirical MNDO-PSDCI calculations have been shown to accurately predict the level ordering in retinal polyenes44,45 and carotenoids.22,46 However, MNDO-PSDCI methods did not provide an adequate model for the ICT state in peridinin.22 Thus, in this study, we included more sophisticated methods. The SAC-CI methods provide the most reliable method for the calculation of excited state dipolar properties, and include the ability to perform excited state minimization with high levels of correlation.26–31,47 All SAC-CI calculations used correlation Level=2 and a double-zeta (D95) basis set.36,43 In addition, coupled-cluster (EOM-CCSD) methods were used to calculate the level ordering with high levels of correlation.32–35 When carrying out EOM-CCSD calculations we used a 32 molecular orbital window consisting of the 16 highest energy filled orbitals and the 16 lowest energy unfilled (virtual) orbitals. The excitation energies and properties were calculated relative to the Møller-Plesset level 2 (MP2) ground state.36 Preliminary calculations demonstrated that this combination worked well for predicting the level ordering in linear polyenes and retinal visual chromophores. All molecular orbital

calculations except for the MNDO-PSDCI procedures were carried out using Gaussian 09.36 The MNDO-PSDCI program is available from R.R. Birge by request.

Results

Steady-state absorption

Steady-state absorption spectra of crocetindial, 8,8'-diapocarotene-8'-ol-8-al and 8,8'-diapocarotene-8,8'-diol in hexane, acetonitrile and methanol are shown in Fig. 2. The spectrum of crocetindial (Fig. 2A) exhibits a red-shift of 8 nm and a broadening of its lineshape upon going from non-polar hexane to the polar solvent, acetonitrile, and a further broadening and additional 2 nm red-shift upon being dissolved in the polar, protic solvent, methanol. Borohydride reduction of one of the conjugated carbonyl groups in crocetindial to form 8,8'-diapocarotene-8'-ol-8-al results in a 6 nm blue-shift of the spectrum taken in hexane compared to that of crocetindial taken in the same solvent. Similarly to crocetindial, dissolving 8,8'-diapocarotene-8'-ol-8-al in methanol and acetonitrile broadens the spectral profiles compared to that seen in hexane, but for this molecule, the spectra do not shift their wavelength positions in the different solvents (Fig. 2B). Reduction of both carbonyls in crocetindial to form 8,8'-diapocarotene-8,8'-diol results in a further 31 nm blue-shift of the spectrum taken in hexane compared to that of 8,8'-diapocarotene-8'-ol-8-al in the same solvent. For 8,8'-diapocarotene-8,8'-diol, however, no solvent dependence of the position of the vibronic bands or lineshape is observed (Fig. 2C). Instead, the spectra in the different solvents coincide almost perfectly except in the region between 300 and 375 nm where significant absorption is evident for the molecule in hexane. This is due to the formation of aggregates caused by the lack of solubility of the polar 8,8'-diapocarotene-8,8'-diol molecule in the non-polar solvent, hexane.

Steady-state fluorescence

Fluorescence spectra of crocetindial, 8,8'-diapocarotene-8'-ol-8-al and 8,8'-diapocarotene-8,8'-diol in hexane, acetonitrile and methanol are shown in Fig. 3. For all three molecules, two different sets of emission spectral bands are observed. The first set displays relatively sharp bands in hexane and is only slightly red-shifted compared to the absorption spectrum. These bands are typical of $S_2 \rightarrow S_0$ emission reported for polyenes and carotenoids.[48–50] The second set of emission bands exhibits a much broader spectral profile, although in some cases (e.g. see Figs. 3B and C) retaining vibronic structure, and is substantially red-shifted relative to their corresponding absorption spectra. This indicates that the emission originates from the S_1 state. For crocetindial dissolved in hexane (Fig. 3A), the $S_2 \rightarrow S_0$ emission bands are most intense whereas in acetonitrile and methanol (Fig. 3B and C), the $S_1 \rightarrow S_0$ emission is more prominent. For 8,8'-diapocarotene-8'-ol-8-al (Fig. 3D–F), the S_1 emission is strongly dominant in all solvents, and the spectrum broadens and loses all vibronic band structure in the polar solvents, methanol and acetonitrile, compared to that seen in hexane. Emission spectra of 8,8'-diapocarotene-8,8'-diol (Fig. 3G and H) taken in acetonitrile and methanol appear at the same wavelength positions and with similar amounts of vibronic structure, but differ slightly in the ratio of S_2 vs. S_1 emission: In acetonitrile the ratio is slightly higher than in methanol. 8,8'-diapocarotene-8,8'-diol was not sufficiently soluble in hexane to obtain a reasonable emission spectrum.

Transient absorption

Transient absorption spectra of crocetindial, 8,8'-diapocarotene-8'-ol-8-al and 8,8'-diapocarotene-8,8'-diol taken in different solvents at various delay times after excitation into the S_2 state are shown in Fig. 4. At time zero (within the time duration of the excitation laser pulse, labeled 0 fs in Fig. 4) the spectra for all three molecules exhibit bleaching of the ground state absorption and a small amount of stimulated fluorescence.

Excitation of crocetindial in all solvents results in a rapid build-up of excited state absorption (ESA) in the wavelength range 450–550 nm (Figs. 4A–C). This build up of ESA is associated with an $S_1 \rightarrow S_n$ transition. The transient absorption spectra taken at delay times of 200 fs and 1 ps are slightly broader than those taken at 100 ps for the molecule dissolved in hexane and acetonitrile. In methanol very little difference in the width of the transient absorption bands is seen at different time delays after the excitation pulse. However, in methanol an additional small transient absorption band is seen at ~610 nm (Fig. 4C). This band may be attributed to transient absorption from S_1 to a low-lying excited state, possibly the one typically denoted as S_3 into which absorption from the ground state becomes allowed upon *trans*-to-*cis* geometric isomerization. This assignment was made previously based on similar observations on several open-chain carotenoids.[51,52] No evidence of this lower-energy band is seen for crocetindial dissolved in either hexane (Fig. 4A) or acetonitrile (Fig. 4B).

Photoexcitation of 8,8'-diapocarotene-8'-ol-8-al into its S_2 state gives rise to substantially more ESA bands (Figs. 4D–F) than seen for crocetindial (Figs. 4A–C). In hexane (Fig. 4D) at a 200 fs time delay, a positive ESA signal appears at 495 nm. This band becomes even stronger in the 10 ps time delay trace and is typical of an $S_1 \rightarrow S_n$ transition observed for carotenoids and polyenes.[51–54] The band appears blue-shifted by ~10 nm compared to the same signal seen in crocetindial in hexane (Fig. 4A). This blue-shift is due to the shorter π-electron conjugation length of 8,8'-diapocarotene-8'-ol-8-al compared to crocetindial (Fig. 1). In addition, two other bands at ~560 and 610 nm that were not present in the 200 fs trace become evident in the 10 ps spectrum of 8,8'-diapocarotene-8'-ol-8-al. These bands are highly reminiscent of those attributed to an ICT $\rightarrow S_n$ transition that is uniquely present in carbonyl-containing polyenes and carotenoids.[9,10,12,13,15,53,55] When 8,8'-diapocarotene-8'-ol-8-al is dissolved in the polar solvents, acetonitrile and methanol (Figs. 4E and F), the ESA lineshape becomes strikingly different compared to that seen in hexane (Fig. 4D). At a 200 fs time delay, three strong bands are observed at ~510, 575 and 730 nm. The band at 730 nm disappears completely from the spectrum taken at a 1 ps time delay suggesting that it is associated with an $S_2 \rightarrow S_n$ transition that decays rapidly as the S_2 state nonradiatively converts to S_1. Of the remaining two bands, the one at 510 nm is sharper than the one at 575 nm and is very likely associated with the same $S_1 \rightarrow S_n$ transition that gives rise to the band at 495 nm in hexane. The apparent red-shift from 495 nm to 510 nm is undoubtedly due to the fact that owing to the broader $S_0 \rightarrow S_2$ spectrum in the polar solvents (Fig. 2B) the negative ground state bleaching signal below 500 nm encroaches on the region of positive amplitude of the $S_1 \rightarrow S_n$ transition and shifts the maximum of the band slightly to longer wavelength. The ESA signal at 575 in acetonitrile and methanol is broad and asymmetric and has a prominent shoulder on the long wavelength side of the band. This shape is most likely due to the merging of at least two separate ESA bands in this wavelength region.

Transient absorption spectra of 8,8'-diapocarotene-8,8'-diol in acetonitrile and methanol are given in Figs. 4G and H. This molecule was not sufficiently soluble in hexane to obtain an ESA spectrum of reasonable quality. In both acetonitrile and methanol, at a 200 fs delay time, two strong ESA bands appear at ~470 nm and 750 nm. The band at 750 nm is broad and completely gone from the spectral traces taken at a 1 ps delay. Therefore, it can be assigned to an $S_2 \rightarrow S_n$ transition. The band at 470 nm is much sharper and once again typical of that seen for $S_1 \rightarrow S_n$ transitions from carotenoids and polyenes. It is blue-shifted by ~40 nm and ~60 nm compared to the same signal observed for 8,8'-diapocarotene-8'-ol-8-al (Fig. 4F) and crocetindial (Fig. 4C), respectively, in methanol. This blue-shift is due to the fact that 8,8'-diapocarotene-8,8'-diol has the shortest π-electron conjugated chain of the molecules examined here.

Kinetics analysis

Transient profiles corresponding to the most prominent bands of the ESA spectra shown in Fig. 4 were fit to a sum of exponentials in order to obtain the excited state dynamics of the molecules. Figure 5 shows the solvent dependence of the decay kinetics of the ESA signals. The solid lines represent the fits obtained from the kinetics analysis. For crocetindial (Fig. 5A), only a small dependence on solvent was observed: The S_1 lifetime being 127 ps in hexane, 135 ps in acetonitrile and 97 ps in methanol. A recent ultrafast transient absorption investigation has been reported for crocin, a diester formed from the disaccharide gentiobiose and the dicarboxylic acid crocetin.56 Crocin has an identical π-electron conjugated chain as crocetindial investigated here, but instead of displaying a 97 ps S_1 lifetime in methanol, it was found to have a lifetime of 135 ps; *i.e.* similar to that observed for crocetindial in hexane and acetonitrile. The lack of an effect of polarity the S_1 lifetime of crocin in methanol was attributed to a partial isolation of the carbonyl groups from the main conjugation due to their involvement as ester linkages to the bulky hydrophilic disaccharide groups.56 However, the decay dynamics of 8,8'-diapocarotene-8'-ol-8-al show an extreme sensitivity to solvent polarity. The lifetime of the excited state is 300 ps in hexane, and shorter by more than an order of magnitude in acetonitrile (21 ps) and methanol (18 ps). These data from crocetindial and 8,8'-diapocarotene-8'-ol-8-al clearly demonstrate the obligatory need for the asymmetric placement of a carbonyl group for such a profound effect of solvent on the excited state lifetime to be observed. It is also important to point out that for 8,8'-diapocarotene-8'-ol-8-al, no dependence of the decay kinetics on the detection wavelength was observed. Figure S1 presents an overlay of the kinetics monitored in the short ($S_1 \rightarrow S_n$) and long (ICT $\rightarrow S_n$) wavelength ESA regions and shows that the kinetic traces are essentially the same within experimental error.

A more detailed kinetics analysis was carried out by globally fitting the entire spectral and temporal datasets using a model based on a sequential decay mechanism. The resulting lineshapes are termed evolution associated difference spectra (EADS) and are given in Fig. 6.

For all three molecules, three EADS components were sufficient to obtain a satisfactory fit based on singular value decomposition (SVD) and minimization of the residual matrix. The fastest kinetic component has a time constant ranging from 120 to 170 fs and contains a number of negative bands in the 450–600 nm range. As mentioned above, these are attributable to a combination of bleaching of the steady-state $S_0 \rightarrow S_2$ absorption bands and stimulated emission from the S_2 state. A second EADS component falls in the range 280 to 900 fs and due to the fact that in all cases it appears much broader than the third EADS component into which it evolves, it is assigned to a vibrationally non-equilibrated S_1 excited state, consistent with previous reports on several different carotenoids.51,52,57–60

The third and final EADS component for crocetindial (Figs. 6A–C) exhibits a strong band between 500 and 525 nm characteristic of a transition from a vibrationally-relaxed S_1 state to a higher S_n excited state. In addition, a smaller amplitude band is present at 610 nm in this component for crocetindial in all solvents, although it is quite weak in hexane. The fact that the strong and weak bands occur in the same EADS component suggests that they originate and are associated with decay from the same (S_1) excited state. The time constant of this component is 127 ps in hexane, 135 ps in acetonitrile, and 97 ps in methanol.

The band profile of the third EADS component for 8,8'-diapocarotene-8,8'-diol in acetonitrile and methanol (Figs. 6G and H) resembles that from crocetindial (Figs. 6B and C) including the presence of a small amplitude band at ~590 nm. However, the lifetime of the third component for 8,8'-diapocarotene-8,8'-diol is much longer than that of crocetindial:

It is 420 ps in acetonitrile and 450 ps in methanol, an effect that can be attributed to the higher S_1 energy of 8,8'-diapocarotene-8,8'-diol compared with crocetindial.

In contrast to crocetindial and 8,8'-diapocarotene-8,8'-diol, the lineshape and lifetime of the third EADS component of 8,8'-diapocarotene-8'-ol-8-al is strongly dependent on solvent polarity. In all solvents the lineshape contains features attributed to both $S_1 \rightarrow S_n$ and ICT $\rightarrow S_n$ transitions with the latter bands appearing at longer wavelength and being much more prominent in the polar solvents, acetonitrile and methanol. Also, as already mentioned above, the lifetime is shorter by more than an order of magnitude in the polar solvents compared to in the non-polar solvent (Figs. 6D–F). Table 1 summarizes the results of all the kinetics analyses.

Discussion

Steady-state absorption and fluorescence

The absorption spectra of crocetindial, 8,8'-diapocarotene-8'-ol-8-al and 8,8'-diapocarotene-8,8'-diol shift systematically to shorter wavelength due to the S_2 state of the molecules becoming higher in energy as the π-electron conjugated chain length is shortened. However, only crocetindial displays an effect of solvent on the wavelength position of its absorption bands (Fig. 2). Figure 2A shows that the absorption spectrum of crocetindial shifts noticeably to longer wavelength in going from hexane to acetonitrile to methanol. This shift occurs despite the fact that the polarizabilities of these solvents decrease slightly in that same order. We cannot provide a definitive explanation of this observation. We suggest that the observed blue-shift may reflect the formation of *s-cis* or corkscrew conformations 51 that enhance the dipole moment of the ground state in polar solvent. The formation of these conformations would preferentially stabilize the ground state and lead to a blue-shift in the absorption spectrum.

The $S_0 \rightarrow S_2$ absorption spectra of crocetindial and 8,8'-diapocarotene-8'-ol-8-al exhibit substantial line-broadening and loss of vibronic resolution when the molecules are dissolved in the polar solvents, acetonitrile and methanol, but 8,8'-diapocarotene-8,8'-diol does not (Fig. 2). The absorption band-broadening is characteristic of carotenoids and polyenes having at least one carbonyl group in conjugation with the π-electron system of carbon-carbon double bonds,[8,10,53,55] and is caused by an ensemble of conformational isomers that forms when the molecules are dissolved in polar solvents. Because each individual isomer has a slightly different absorption spectrum, the distribution results in a heterogeneously broadened band envelope.[22,61] Spectral broadening with increasing solvent polarity is also observed in the $S_1 \rightarrow S_0$ fluorescence spectra of 8,8'-diapocarotene-8'-ol-8-al (Fig. 3D–F), but not for crocetindial (Fig. 3A–C) or 8,8'-diapocarotene-8,8'-diol (Fig. 3G and H). This broadening indicates that, unlike the molecules in the S_2 state which form a broad distribution of conformational isomers in polar solvents when either one or two carbonyls are present in the π-electron conjugation, the molecules in the S_1 state will only do so when one carbonyl is present. Somehow the presence of two terminal carbonyls in crocetindial, perhaps due to their symmetric placement, leads to a narrower potential energy well in the S_1 state that inhibits the formation of conformational isomers compared to that of its S_2 state. The apparent propensity for 8,8'-diapocarotene-8'-ol-8-al to undergo conformational twisting in both the S_1 and S_2 states may be related to its ability to form an ICT state as discussed further below.

All three of the molecules investigated here display some amount of emission from both the S_1 and S_2 states, but only crocetindial exhibits a clear crossover from dominant S_2 emission (Fig. 3A) to dominant S_1 emission (Figs. 3B and C) upon transferring the molecule from the non-polar solvent, hexane, to either of the polar solvents, acetonitrile or methanol. A similar

crossover has been reported for carotenoids with decreasing conjugated chain lengths.[49,62] Carotenoids with nine or more carbon-carbon double bonds show primarily fluorescence associated with the $S_2 \rightarrow S_0$ transition. For shorter-chromophore carotenoids, the fluorescence is dominated by the $S_1 \rightarrow S_0$ transition. This crossover has been explained by a smaller S_2 - S_1 energy gap in the shorter molecules which promotes nonradiative internal conversion from S_2 leading to a diminished yield of fluorescence from the S_2 state.[5,49,63] For longer carotenoids ($N \geq 9$) which have larger S_2 - S_1 energy gaps, the rate of $S_2 \rightarrow S_1$ internal conversion is decreased, and this enhances the probability of S_2 emission. For crocetindial, the fact that there is a red-shift of the $S_2 \rightarrow S_0$ absorption spectrum in going from hexane to acetonitrile (Figs. 2A) while the S_1 lifetime remains essentially constant for these samples (Fig. 5A) indicates that the S_2 - S_1 energy gap is indeed smaller in acetonitrile compared to in hexane. Thus, an increased rate of $S_2 \rightarrow S_1$ internal conversion accompanied by a diminished probability of S_2 emission in the polar solvent is expected and observed (Figs. 3A and B).

Excited state spectra and kinetics

The wavelengths of the ESA spectral features and the dynamics for all three molecules can be accounted for on the basis of changes in the energies of the S_1, S_2 and ICT excited states as a function of N and solvent polarity. As the π-electron chain length of the molecules decreases with the removal of a carbonyl from the conjugated system, the S_1 state energy decreases faster than the S_n state, resulting in a blue-shift of the $S_1 \rightarrow S_n$ ESA band position. For 8,8'-diapocarotene-8'-ol-8-al, as the polarity of the solvent increases in going from hexane to acetonitrile or methanol, the ICT state is stabilized and the excited state lifetime of the molecule becomes shorter. It is important to point out, however, that unlike other carbonyl-containing carotenoids and polyenes,[11,53] 8,8'-diapocarotene-8'-ol-8-al exhibits no effect of probe wavelength on the dynamics of the excited state (Fig. S1) suggesting that either the S_1 and ICT states are strongly coupled or that the populations of the states exist in fast equilibrium.

The most striking observation in the kinetics data is that the excited state lifetime of the asymmetric 8,8'-diapocarotene-8'-ol-8-al molecule is profoundly dependent on solvent polarity whereas the symmetric crocetindial and 8,8'-diapocarotene-8,8'-diol molecules are not. This observation follows from the fact that 8,8'-diapocarotene-8'-ol-8-al has a large ground state dipole moment, and that the two lowest-lying ππ* excited singlet states involve varying degrees of charge-transfer character. Solvent effects on both level ordering and excited state properties are of critical importance in the evolution of these singlet states, which depends on the polarity of the solvent. We now proceed to discuss this issue in detail.

Molecular orbital theory and molecular dynamics

Presented here is an overview of the molecular orbital calculations with an emphasis on understanding the nature of the ICT state. Additional details regarding the calculations can be found in the supplementary information.

Excited state level ordering

The photophysical properties of crocetindial, 8,8'-diapocarotene-8'-ol-8-al, and 8,8'-diapocarotene-8,8'-diol are determined in large part by the excited singlet state level ordering. In vacuum or non-polar solvents, all three compounds have lowest-lying 2^1A_g-like excited singlet states (see discussion above). Previous theoretical studies have demonstrated that the description of such states requires doubly excited configuration interaction, or procedures with comparable levels of correlation.[64,65] The calculated level orderings based on MNDO-PSDCI and EOM-CCSD calculations are shown in Fig. 7. Each excited state is represented by a rectangle, the vertical width of which is proportional to the oscillator

strength, which is a measure of the allowedness of the transition. The color of the rectangle reflects the ionic (red) versus covalent (blue) character of the excited state (see color gauge insert).

The terms ionic and covalent trace their origins to valence bond theory, but both types of states can be properly described using molecular orbital theory provided both single and double configuration interaction (CI) is included. An ionic state is one which is well described by single CI and which tends to have regions of localized charge. Charge transfer states are by definition ionic states. A covalent state is defined by high levels of double CI and a smooth distribution of electron density that minimizes electron-electron repulsion. Such states are said to be well correlated, which means the electrons occupy wavefunctions that distribute the electrons to rigorously minimize repulsion. The ionic and covalent states are pure only in non-polar, symmetrical molecules, such as linear polyenes. In polar molecules, these states are mixed in character, but as can be seen by reference to Fig. 7, the core characteristics remain intact. Note that only 8,8'-diapocarotene-8'-ol-8-al has a static dipole moment.

Nature of the ICT state

One of the key experimental observations of this study is that 8,8'-diapocarotene-8'-ol-8-al exhibits an ICT state in polar solvent. The ICT state in 8,8'-diapocarotene-8'-ol-8-al is qualitatively similar to the ICT state observed in peridinin.9،20،53،66 Because 8,8'-diapocarotene-8'-ol-8-al is significantly smaller, it provides an excellent theoretical target for studying the nature of the ICT state in general. We utilized SAC-CI to examine the dipolar properties of the low-lying excited singlet state of 8,8'-diapocarotene-8'-ol-8-al for three geometries: ground state, relaxed excited state and a 20 fs dynamic state. The last of these is described in a separate section below. SAC-CI methods are one of the best methods available for the calculation of excited state geometries and electron densities.26،29 The SAC-CI method has one flaw, however. Because the double configuration interaction does not include coupled triplets, the ^1B_u-like state is often calculated to be lower in energy than the 2^1A_g-like state in long chain polyenes, contrary to experimental observation. Coupled triplets are important contributors to electron correlation in ^1A_g-like covalent excited singlet states.67 Despite that complication, a great deal can be learned about the ICT state from an analysis of the SAC-CI results.

The dipolar properties of the low-lying singlet states based on the ground state geometry are shown in Fig. 8. Solvent effect calculations indicate that the lowest singlet state would be the ^1A_g-like covalent state, which is S_3 in this diagram. In very polar solvents such as acetonitrile and methanol, the ^1B_u-like ionic state is the lowest excited singlet state (S_1 in this figure). The S_2 state is the nπ^* state, and it is predicted to be above both of these states by more accurate level ordering calculations (see Fig. 7). The S_1 ionic state has properties that are characteristic of the charge transfer state. Of key importance is the large static dipole moment (~20D), which is in the same direction as the ground state dipole moment. The latter is important because it is the ground state that establishes the solvent reaction field upon excitation. Upon excitation, molecules with dipole moments in the same direction as the ground state will be stabilized by this reaction field, which is why the ^1B_u-like ionic state is the lowest singlet state in polar solvent. The other states shown in Fig. 8 have dipole moments that are opposed to the reaction field. These states will all be destabilized in polar solvent. CIS-PCM state-specific solvent effect calculations39،42 indicate that the ^1B_u-like ionic state of 8,8'-diapocarotene-8'-ol-8-al will be stabilized by 0.97 eV in methanol. Solvent destabilization of the ^1A_g-like covalent state is sufficient to invert the lowest two levels shown in Fig. 8. This evidence supports the conclusion that the ^1B_u-like ionic state of 8,8'-diapocarotene-8'-ol-8-al is the lowest-lying excited singlet state in methanol.

A lowest-lying singlet state will live long enough to interact with the reaction field and change geometry on a time scale comparable to the emission process (~1 ps). Geometry changes are driven by the change in orbital occupation, and for polyenes, excitation induces significant bond order reversal. Geometry changes that take place within 0–50 fs; i.e. within the temporal resolution of our spectrometer, and during which time as noted above, the ICT state forms, are of particular interest. To explore the ICT state in more detail, we used SAC-CI methods to generate the equilibrium geometry of the S_1 excited state in vacuum, and used the force constants for the ground and excited states to carry out molecular dynamics using the Charmm forcefield.68 These classical calculations allow explicit inclusion of the solvent, which was assumed to be water, rather than methanol, for simplicity. Twenty 200 fs simulations were run with alternating initial conditions and a time resolution of 0.01 fs. In half of the trajectories, the atoms were started out at rest with random velocities equivalent to the ambient temperature kinetic energy. In the other half, the atoms were started with random positions such that the total potential energy was equal to RT at room temperature. The trajectories were monitored and graphed in terms of RMS deviation from the ground and excited state equilibrium geometries. A plot of the RMS deviations as a function of time is shown in Fig. S3. The equilibrium ground and excited state geometries and the average S_1 geometry after 20 fs are shown in Fig. 9. We assign the S_1 (20 fs) geometry to be our best representation of the ICT state, and we will now call this representation ICT (20 fs). The difference in geometry of this state and the ground state is extremely small and involves primarily small movements in the carbon atoms near the center of the polyene chain. Nevertheless, this geometry exhibits significant bond order reversal and has interesting properties.

The electronic and dipolar properties of the ICT (20 fs) state are presented in Fig. 10. This state exhibits a very large dipole moment (27.9 D) and a large oscillator strength (f = 2.24). The calculated transition energy of 2.24 eV is close to the experimental transition energy of 2.37 eV estimated based on the origin reflected emission spectrum (see Fig. S2). A key observation is that the configurational characteristics of this state include a large (16%) contribution from double excited configurations. Indeed, this state shares significant configurational character with the higher energy 2^1A_g-like covalent state, and can be viewed as a linear combination of the 1^1B_u-like ionic and 2^1A_g-like covalent states. The charge-transfer character is due to a selection of those configurations from both parent states, which enhance the dipole moment of the final state. We believe this statement is true of all ICT states reported for carbonyl-containing polyenes and carotenoid. Namely, the creation of a lowest-lying ICT state requires extensive mixing of the lowest-lying 1^1B_u-like ionic and 2^1A_g-like covalent states to form a new state with extensive bond order reversal and charge transfer character. Recall that extensive bond order reversal is normally a characteristic of covalent states and charge transfer is normally a characteristic of ionic states. The ICT state is a charge-transfer (ionic-like) state with extensive (covalent-like) bond order reversal.

Our choice of the 20 fs dynamic state is not a key decision. SAC-CI calculations were run for the 50 and 100 fs states with nearly identical results to those shown in Fig. 10. The dynamic oscillations observed in Fig. S3 involve carbon-carbon conjugated (double and single) bond stretching modes and each oscillation translates to a change in total transition energy of about 0.08 eV. This observation would by itself account for the broadness observed in the emission spectrum. But solvent relaxation processes in the ICT state would also contribute to spectral inhomogeneity, and thus there are at least two important sources generating broad emission and $S_{ICT} \rightarrow S_n$ spectra.

Conclusions

In this work we have carried out femtosecond time-resolved optical spectroscopic experiments on crocetindial, 8,8'-diapocarotene-8'-ol-8-al, and 8,8'-diapocarotene-8,8'-diol to investigate the nature and origin of the ICT state in carbonyl-containing carotenoids and polyenes. The data show that only the asymmetrically substituted 8,8'-diapocarotene-8'-ol-8-al exhibits any substantial effect of solvent on the excited state spectra and dynamics that indicate the presence of an ICT state. The spectroscopic data are interpreted using molecular orbital theory and molecular dynamics calculations which show that the ICT state evolves in polar solvent via mixing of the low-lying S_1 (2^1A_g-like) and S_2 (1^1B_u-like) excited singlet states and arises in ~20 fs as a resultant state that exhibits a very large (~25D) dipole moment.

Supplementary Material

Refer to Web version on PubMed Central for supplementary material.

Acknowledgments

The authors wish to thank Dr. Razi Naqvi for the generous gift of the crocetindial and Dr. Tomáš Polívka for many useful discussions. This work has been supported in the laboratory of HAF by grants from the National Science Foundation (MCB-0913022) and the University of Connecticut Research Foundation. The work in the laboratory of RRB was supported by grants from the National Institutes of Health (GM-34548) and the National Science Foundation (EMT-08517).

References

1. Pariser R. J. Chem. Phys. 1955; 24:250.
2. Hudson B, Kohler B. Ann. Rev. Phys. Chem. 1974; 25:437.
3. Callis PR, Scott TW, Albrecht AC. J. Chem. Phys. 1983; 78:16.
4. Birge RR. Accts. Chem. Res. 1986; 19:138.
5. Christensen RL, Barney EA, Broene RD, Galinato MGI, Frank HA. Arch. Biochem. Biophys. 2004; 430:30. [PubMed: 15325909]
6. Hudson BS, Kohler BE. J. Chem. Phys. 1973; 59:4984.
7. Hudson, BS.; Kohler, BE.; Schulten, K. Linear polyene electronic structure and potential surfaces. In: Lim, ED., editor. Excited States. Vol. Vol. 6. New York: Academic Press; 1982. p. 1
8. Polívka T, Sundström V. Chem. Rev. 2004; 104:2021. [PubMed: 15080720]
9. Bautista JA, Connors RE, Raju BB, Hiller RG, Sharples FP, Gosztola D, Wasielewski MR, Frank HA. J. Phys. Chem. B. 1999; 103:8751.
10. Frank HA, Bautista JA, Josue J, Pendon Z, Hiller RG, Sharples FP, Gosztola D, Wasielewski MR. J. Phys. Chem. B. 2000; 104:4569.
11. Wild DA, Winkler K, Stalke S, Oum K, Lenzer T. Phys. Chem. Chem. Phys. 2006; 8:2499. [PubMed: 16721434]
12. Ehlers F, Wild DA, Lenzer T, Oum K. J. Phys. Chem. A. 2007; 111:2257. [PubMed: 17388322]
13. Kopczynski M, Ehlers F, Lenzer T, Oum K. J. Phys. Chem. A. 2007; 111:5370. [PubMed: 17550237]
14. Stalke S, Wild DA, Lenzer T, Kopczynski M, Lohse PW, Oum K. Phys. Chem. Chem. Phys. 2008; 10:2180. [PubMed: 18404224]
15. Chatterjee N, Niedzwiedzki DM, Kajikawa T, Hasegawa S, Katsumura S, Frank HA. Chem. Phys. Lett. 2008; 463:219. [PubMed: 19777053]
16. Vaswani HM, Hsu CP, Head-Gordon M, Fleming GR. J. Phys. Chem. B. 2003; 107:7940.
17. Papagiannakis E, Larsen DS, van Stokkum IHM, Vengris M, Hiller RG, van Grondelle R. Biochem. 2004; 43:15303. [PubMed: 15581342]

18. Papagiannakis E, Vengris M, Larsen DS, van Stokkum IHM, Hiller RG, van Grondelle R. J. Phys. Chem. B. 2006; 110:512. [PubMed: 16471563]
19. Van Tassle AJ, Prantil MA, Hiller RG, Fleming GR. Is. J. Chem. 2007; 47:17.
20. Zigmantas D, Hiller RG, Yartsev A, Sundström V, Polivka T. J. Phys. Chem. B. 2003; 107:5339.
21. Linden PA, Zimmermann J, Brixner T, Holt NE, Vaswani HM, Hiller RG, Fleming GR. J. Phys. Chem. B. 2004; 108:10340.
22. Shima S, Ilagan RP, Gillespie N, Sommer BJ, Hiller RG, Sharples FP, Frank HA, Birge RR. J. Phys. Chem. A. 2003; 107:8052.
23. Ilagan RP, Koscielecki JF, Hiller RG, Sharples FP, Gibson GN, Birge RR, Frank HA. Biochem. 2006; 45:14052. [PubMed: 17115700]
24. Ziólek M, Lorenc M, Naskrecki R. Appl. Phys. B. 2001; 72:843.
25. Martin CH, Birge RR. J. Phys. Chem. A. 1998; 102:852.
26. Ishida M, Toyota K, Ehara M, Frisch MJ, Nakatsuji H. The Journal of Chemical Physics. 2004; 120:2593. [PubMed: 15268403]
27. Miyahara T, Tokita Y, Nakatsuji H. J. Phys. Chem. B. 2001; 105:7341.
28. Miyahara T, Nakatsuji H, Hasegawa J, Osuka A, Aratani N, Tsuda A. J. Chem. Phys. 2002; 117:11196.
29. Nakajima T, Nakatsuji H. Chem. Phys. 1999; 242:177.
30. Nakatsuji H. Chem. Phys. Lett. 1978; 59:362.
31. Nakatsuji H. Chem. Phys. Lett. 1991; 177:331.
32. Koch H, Jørgensen P. J. Chem. Phys. 1990; 93:3333.
33. Stanton JF, Bartlett RJ. J. Chem. Phys. 1993; 98:7029.
34. Koch H, Kobayashi R, Sánchez de Merás A, Jørgensen P. J. Chem. Phys. 1994; 100:4393.
35. Kállay M, Gauss J. J. Chem. Phys. 2004; 121:9257. [PubMed: 15538846]
36. Frisch, MJT.; G, W.; Schlegel, HB.; Scuseria, GE.; Robb, MA.; Cheeseman, JR.; Scalmani, G.; Barone, V.; Mennucci, B.; Petersson, GA.; Nakatsuji, H.; Caricato, M.; Li, X.; Hratchian, HP.; Izmaylov, AF.; Bloino, J.; Zheng, G.; Sonnenberg, JL.; Hada, M.; Ehara, M.; Toyota, K.; Fukuda, R.; Hasegawa, J.; Ishida, M.; Nakajima, T.; Honda, Y.; Kitao, O.; Nakai, H.; Vreven, T.; Montgomery, JA., Jr; Peralta, JE.; Ogliaro, F.; Bearpark, M.; Heyd, JJ.; Brothers, E.; Kudin, KN.; Staroverov, VN.; Kobayashi, R.; Normand, J.; Raghavachari, K.; Rendell, A.; Burant, JC.; Iyengar, SS.; Tomasi, J.; Cossi, M.; Rega, N.; Millam, NJ.; Klene, M.; Knox, JE.; Cross, JB.; Bakken, V.; Adamo, C.; Jaramillo, J.; Gomperts, R.; Stratmann, RE.; Yazyev, O.; Austin, AJ.; Cammi, R.; Pomelli, C.; Ochterski, JW.; Martin, RL.; Morokuma, K.; Zakrzewski, VG.; Voth, GA.; Salvador, P.; Dannenberg, JJ.; Dapprich, S.; Daniels, AD.; Farkas, ö.; Foresman, JB.; Ortiz, JV.; Cioslowski, J.; Fox, DJ. Wallingford CT: Gaussian, Inc.; 2009. Gaussian 09. Revision A.1. Wallingford CT: Gaussian, Inc.; 2009.
37. Barone V, Cossi M, Tomasi J. J. Comput. Chem. 1998; 19:404.
38. Wang LY, Chen QW, Zhai GH, Wen ZY, Zhang ZX. Journal of Molecular Structure: THEOCHEM. 2006; 778:15.
39. Tomasi J, Mennucci B, Cammi R. Chem. Rev. 2005; 105:2999. [PubMed: 16092826]
40. York DM, Karplus M. J. Phys. Chem. A. 1999; 103:11060.
41. Improta R, Scalmani G, Frisch MJ, Barone V. J. Chem. Phys. 2007; 127:1.
42. Cossi M, Rega N, Scalmani G, Barone V. J. Comp. Chem. 2003; 24
43. Dunning, TH., Jr; Hay, PJ. Modern Theoretical Chemistry. In: Schaefer, HF., editor. Modern Theoretical Chemistry. Vol. Vol. 3. New York: Plenum, New York; 1976. p. 1
44. Ren L, Martin CH, Wise KJ, Gillespie NB, Luecke H, Lanyi JK, Spudich JL, Birge RR. Biochem. 2001; 40:13906. [PubMed: 11705380]
45. Dukkipati A, Kusnetzow A, Babu KR, Ramos L, Singh D, Knox BE, Birge RR. Biochem. 2002; 41:9842. [PubMed: 12146950]
46. Pendon ZD, Sullivan JO, van der Hoef I, Lugtenburg J, Cua A, Bocian DF, Birge RR, Frank HA. Photosynth. Res. 2005; 86:5. [PubMed: 16172922]
47. Nakatsuji H, Hirao K. J. Chem. Phys. 1978; 68:2053.

48. Christensen RL, Goyette M, Gallagher L, Duncan J, DeCoster B, Lugtenburg J, Jansen FJ, Hoef Ivd. J. Phys. Chem. A. 1999; 103:2399.
49. Frank HA, Josue JS, Bautista JA, van der Hoef I, Jansen FJ, Lugtenburg J, Wiederrecht G, Christensen RL. J. Phys. Chem. B. 2002; 106:2083.
50. Christensen RL, Galinato MGI, Chu EF, Howard JN, Broene RD, Frank HA. J. Phys. Chem. A. 2008; 112:12629. [PubMed: 19007144]
51. Niedzwiedzki D, Koscielecki JF, Cong H, Sullivan JO, Gibson GN, Birge RR, Frank HA. J. Phys. Chem. B. 2007; 111:5984. [PubMed: 17441762]
52. Niedzwiedzki DM, Sandberg DJ, Cong H, Sandberg MN, Gibson GN, Birge RR, Frank HA. Chem. Phys. 2009; 357:4.
53. Niedzwiedzki DM, Chatterjee N, Enriquez MM, Kajikawa T, Hasegawa S, Katsumura S, Frank HA. J. Phys. Chem. B. 2009; 113:13604. [PubMed: 19775150]
54. Niedzwiedzki DM, Enriquez MM, LaFountain AM, Frank HA. Chem. Phys. 2010; 373:80. [PubMed: 20689726]
55. Zigmantas D, Hiller RG, Sharples FP, Frank HA, Sundström V, Polivka T. Phys. Chem. Chem. Phys. 2004; 6:3009.
56. Chábera P, Fuciman M, Razi Naqvi K, Polivka T. Chem. Phys. 2010; 373:56.
57. Niedzwiedzki DM, Sullivan JO, Polivka T, Birge RR, Frank HA. J. Phys. Chem. B. 2006; 110:22872. [PubMed: 17092039]
58. Billsten HH, Zigmantas D, Sundström V, Polívka T. Chem. Phys. Lett. 2002; 355:465.
59. de Weerd FL, van Stokkum IHM, van Grondelle R. Chem. Phys. Lett. 2002; 354:38.
60. Pendon ZD, Gibson GN, van der Hoef I, Lugtenburg J, Frank HA. J. Phys. Chem. B. 2005; 109:21172. [PubMed: 16853743]
61. Christensen RL, Kohler BE. Photochem. Photobiol. 1973; 18:293.
62. DeCoster B, Christensen RL, Gebhard R, Lugtenburg J, Farhoosh R, Frank HA. Biochim. Biophys. Acta. 1992; 1102:107. [PubMed: 1510992]
63. Christensen RL, Galinato MGI, Chu EF, Fujii R, Hashimoto H, Frank HA. J. Am. Chem. Soc. 2007; 129:1769. [PubMed: 17284007]
64. Birge RR, Pierce BM. J. Chem. Phys. 1979; 70:165.
65. Birge R, Bennett J, Hubbard L, Fang H, Pierce B, Kliger D, Leroi G. J. Am. Chem. Soc. 1982; 104:2519.
66. Zigmantas D, Polivka T, Hiller RG, Yartsev A, Sundström V. J. Phys. Chem. A. 2001; 105:10296.
67. Schulten K, Ohmine I, Karplus M. J. Chem. Phys. 1976; 64:4422.
68. Brooks B, Bruccoleri RE, Olafson BD, States DJ, Swaminathan S, Karplus M. J. Comp. Chem. 1983; 4:187.

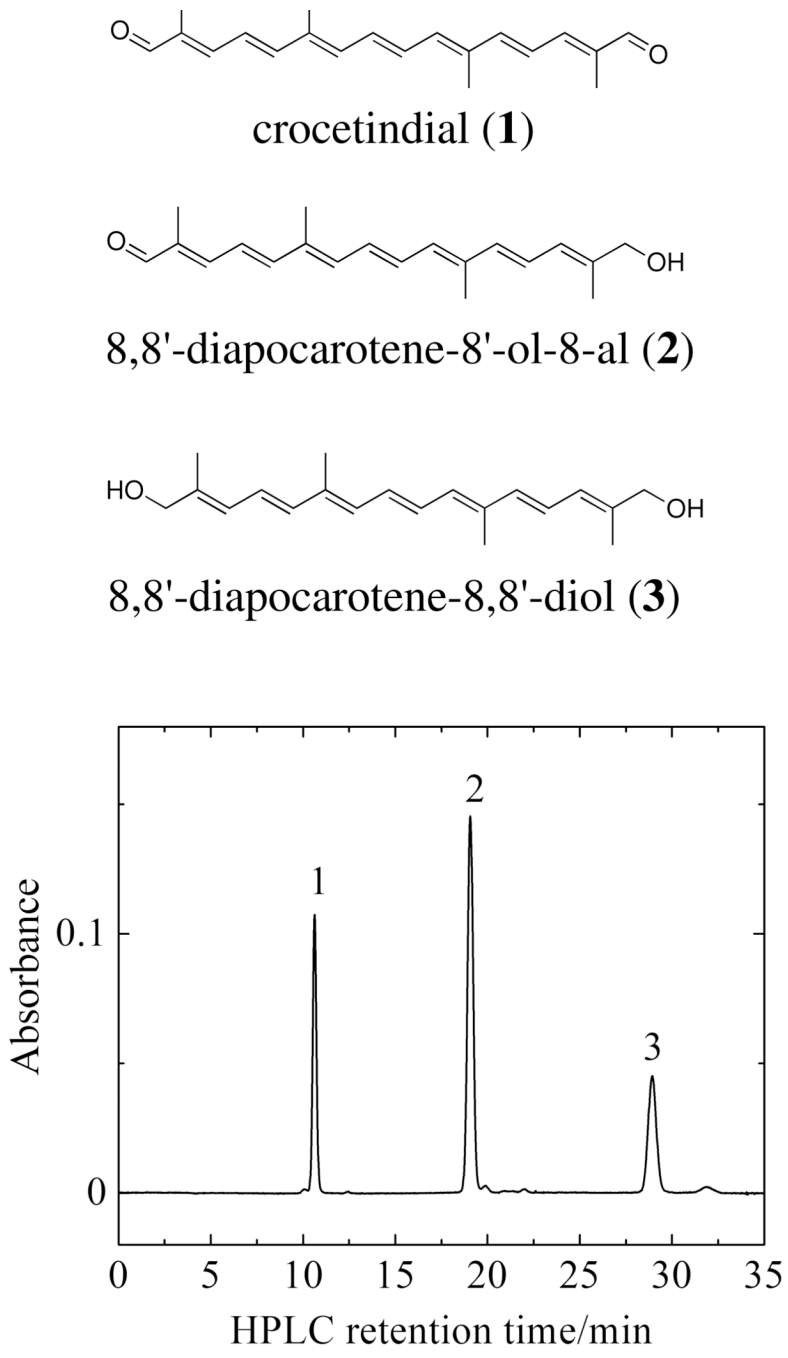

Figure 1.
Structures and HPLC chromatogram of crocetindial, 8,8'-diapocarotene-8'-ol-8-al and 8,8'-diapocarotene-8,8'-diol.

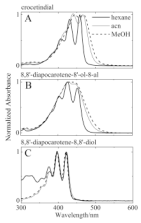

Figure 2.
Steady-state absorption spectra of crocetindial, 8,8'-diapocarotene-8'-ol-8-al and 8,8'-diapocarotene-8,8'-diol recorded in hexane, acetonitrile (acn), and methanol (MeOH) at room temperature.

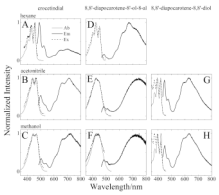

Figure 3.

Fluorescence emission spectra of crocetindial, 8,8'-diapocarotene-8'-ol-8-al and 8,8'-diapocarotene-8,8'-diol taken in different solvents at room temperature. All spectra were normalized.

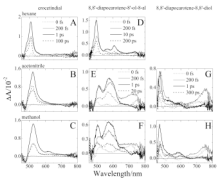

Figure 4.
Transient absorption spectra of crocetindial, 8,8'-diapocarotene-8'-ol-8-al and 8,8'-diapocarotene-8,8'-diol taken at different time delays after excitation at 406 nm in different solvents at room temperature.

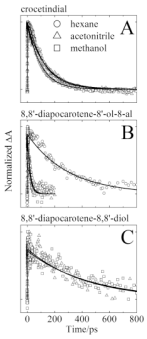

Figure 5.
Representative kinetic traces (symbols) with fits obtained at maxima of S_1 - S_n bands (single wavelengths) (lines). All kinetic traces were normalized for clarity.

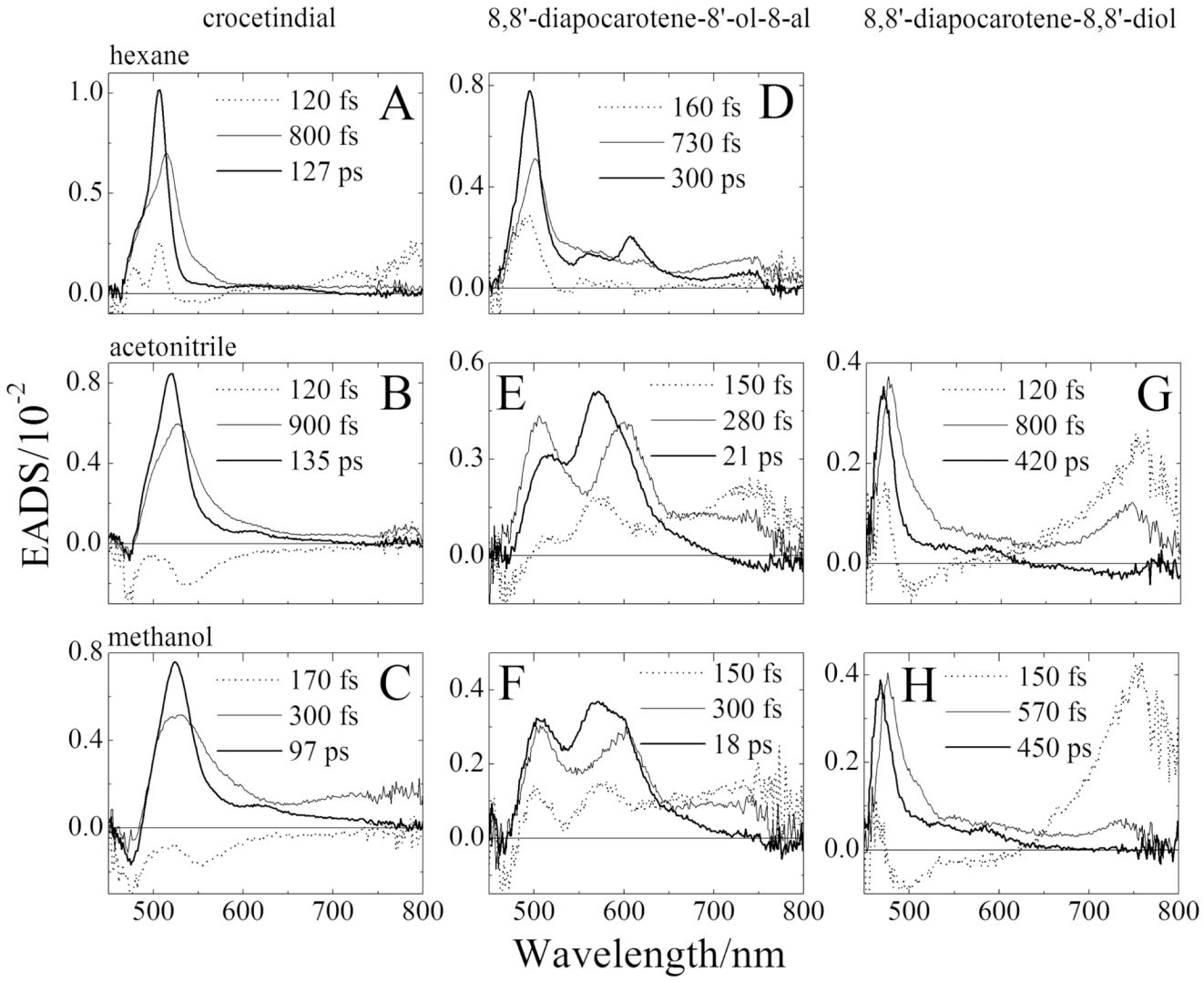

Figure 6.
Evolution associated difference spectra (EADS) obtained from global fitting results of the transient absorption in Fig. 4.

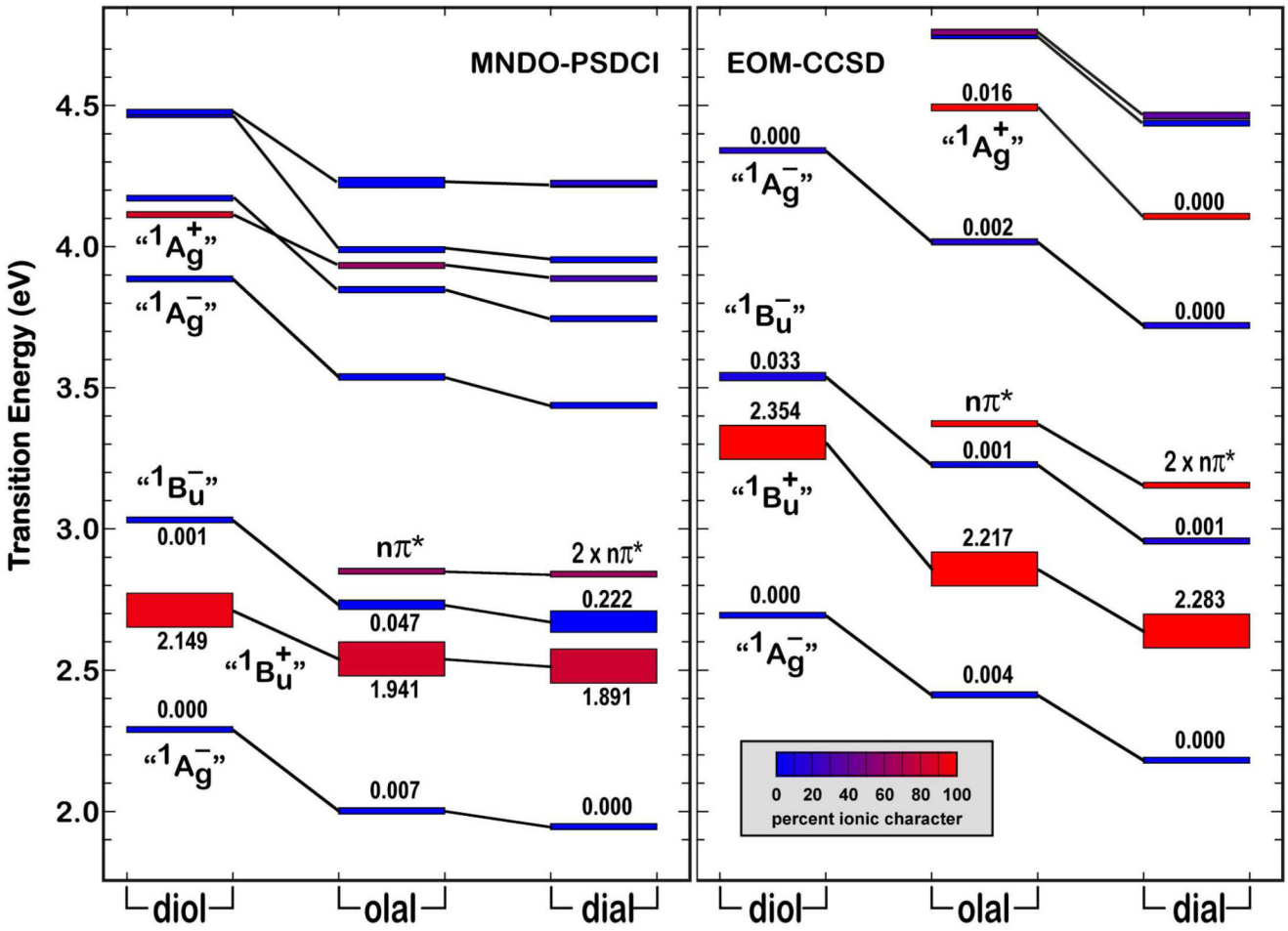

Figure 7.

Calculated electronic properties of the low-lying excited singlet states of crocetindial (dial), 8,8'-diapocarotene-8'-ol-8-al (olal), and 8,8'-diapocarotene-8,8'-diol (diol) based on MNDO-PSDCI and EOM-CCSD molecular orbital theory (see text). The oscillator strengths of selected states are printed above or below the state rectangles, the colors of which indicate the percent ionic character based on the inserted gauge. Both methods agree on the level ordering of the first 4–5 states, and agree reasonably well with the Franck-Condon maxima of the various spectra (see Fig. S2).

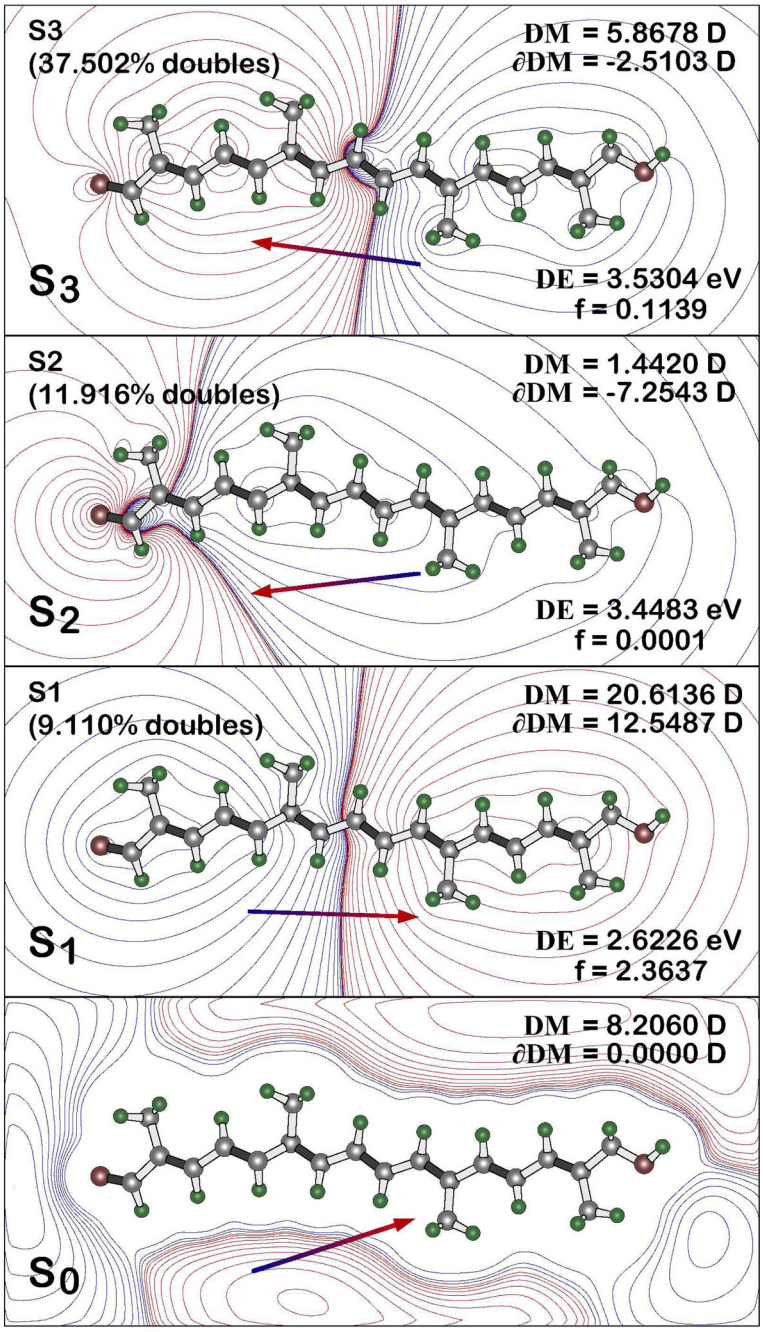

Figure 8.

SAC-CI analysis of the dipolar properties of the low-lying singlet states in 8,8'-diapocarotene-8'-ol-8-al based on the equilibrium ground state geometry. The contours and the arrow in the lowest (S_0) panel reflect the ground state dipolar properties. The contours and the arrows in the S_1; S_2 and S_3 panels reflect the charge shifts upon excitation into these states. The ground electrostatic field and the excited state charge shift contours are approximate and are calculated assuming vacuum conditions and point-charge electrostatics with contour levels: 0; ±173; ±1380; ± 4680; ±11,100; ±21,700; ±37,500; ±59,500; ±88,900; ±126,000; ±173,000; ±231,000; ±300,000; ±381,000; ±476,000; ±586,000 J/mol. Blue

contours signify regions of excess negative charge and red contours signify regions of excess positive charge.

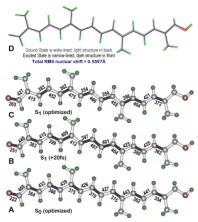

Figure 9.

The ground (A) and excited state (B, C) geometries of 8,8'-diapocarotene-8'-ol-8-al. The ground state geometry was generated using B3LYP/6-31G(d) procedures. The optimized excited state geometry in C was generated using SAC-CI/D95 procedures, and is overlaid on top of the ground state geometry in D. The structure shown in B was generated using Charmm dynamics based on the SAC-CI force constants (see text). Bond lengths of key bonds are indicated next to the bond using the formula (bond length(Å) – 1.0Å) times 1000. Thus a value of 222 indicates a bond length of 1.222Å.

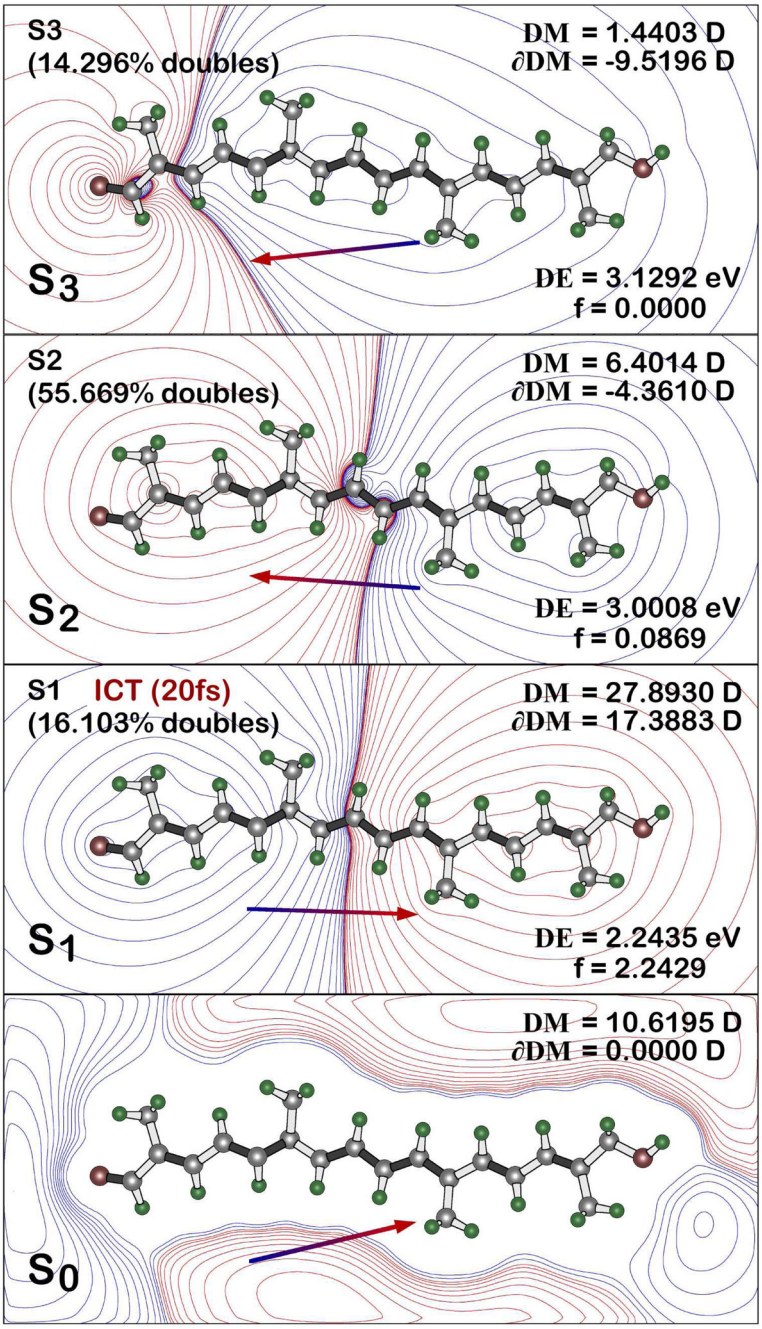

Figure 10.
SAC-CI analysis of the dipolar properties of the low-lying singlet states in 8,8'-diapocarotene-8'-ol-8-al based on the 20 fs geometry shown in panel B of Fig. 9. The ground electrostatic field and the excited state charge shift contours are drawn as in Fig. 8.

Table 1

Dynamics of the excited states of crocetindial, 8,8'-diapocarotene-8'-ol-8-al and 8,8'-diapocarotene-8,8'-diol. The uncertainties in the numbers were determined from an examination of the region of solution for each fitted parameter based on the values of the residuals. The pump wavelength for all samples was set at 406 nm.

molecule	solvent	lifetime		
		τ_1/fs	τ_2/fs	τ_3/ps
crocetindial	hexane	< 170	800 ± 400	127 ± 5
	acetonitrile	< 170	900 ± 500	135 ± 5
	methanol	170 ± 50	300 ± 100	97 ± 5
8,8'-diapocarotene-8'-ol-8-al	hexane	< 170	730 ± 200	300 ± 20
	acetonitrile	< 170	280 ± 50	21 ± 3
	methanol	< 170	300 ± 100	18 ± 2
8,8'-diapocarotene-8,8'-diol	hexane	n.d.	n.d.	n.d.
	acetonitrile	< 170	800 ± 400	420 ± 50
	methanol	< 170	570 ± 300	450 ± 50

n.d. = not determined